

## Bandwidth enhancement and miniaturization of circular-shaped microstrip antenna based on beveled half-cut structure for MIMO 2×2 application

Teguh Firmansyah<sup>1</sup>, Supriyanto Praptodiyono<sup>2</sup>, Herudin<sup>3</sup>, Didik Aribowo<sup>4</sup>, Syah Alam<sup>5</sup>, Dian Widi Astuti<sup>5</sup>, Muchamad Yunus<sup>7</sup>

<sup>1,2,3</sup>Department of Electrical and Engineering, Universitas Sultan Ageng Tirtayasa, Indonesia

<sup>4</sup>Department of Electrical Engineering Vocational Education, Universitas Sultan Ageng Tirtayasa, Indonesia

<sup>5</sup>Department of Electrical Engineering, Universitas 17 Agustus 1945 Jakarta, Indonesia

<sup>6</sup>Department of Electrical Engineering, University of Mercu Buana, Indonesia

<sup>7</sup>Department of Electrical Engineering, University of Pakuan, Indonesia

### Article Info

#### Article history:

Received Aug 6, 2018

Revised Nov 16, 2018

Accepted Dec 26, 2018

#### Keywords:

Antenna  
Bandwidth  
Beveled  
Microstrip  
MIMO

### ABSTRACT

In this paper, circular-shaped microstrip antenna was simulated, fabricated, and measured accordingly. As the novelty, to enhance bandwidth and reduce antenna size, beveled half-cut microstrip structure is proposed. Further, this proposed antenna structure will be applied to multiple input multiple output (MIMO) antenna 2×2. Therefore, this research was investigated conventional circular shape antenna (CCSA), circular shaped beveled antenna (CSBA), and MIMO circular shaped beveled antenna (MIMO-CBSA) as Model 1, Model 2, and Model 3, respectively. An FR4 substrate with  $\epsilon_r=4.4$ , thickness  $h=1.6$  mm, and  $\tan \delta=0.0265$  was used. The simulation has been conducted using Advanced Design System (ADS). The antenna CCSA/CSBA/MIMO-CBSA achieve 1.831GHz/2.265 GHz/2.256 GHz, -15.13dB/-17.37dB/-17.25 dB, 1.42/1.31/1.33, and 1.474/2.332/2.322 for center frequency, reflection coefficient, VSWR, and bandwidth, respectively. This antenna has a size 63x90 mm and 51.5x90 mm for CCSA (Model 1) and CSBA (Model 2), respectively. After the structure of MIMO 2×2 was applied, the size of antenna MIMO-CBSA (Model 3) became 180 mm x 180 mm with a mutual coupling ( $S_{21}$ )=-26.18 dB and mutual coupling ( $S_{31}$ )=-26.41 dB. The result showed that proposed antenna CSBA (Model 2) has wider-bandwidth of 58,2% and smaller-size of 18,2%. Furthermore, after CSBA (Model 2) structure was applied to MIMO 2×2 (Model 3) and the MIMO antenna obtain good mutual coupling (<-15dB). Moreover, the measured results are good agreement with the simulated results. In conclusion, all of these advantages make it particularly valuable in multistandard antenna applications design such as GSM950, WCDMA1800, LTE2300, and WLAN2400.

Copyright © 2019 Institute of Advanced Engineering and Science.  
All rights reserved.

### Corresponding Author:

Teguh Firmansyah,  
Department of Electrical and Engineering,  
University of Sultan Ageng Tirtayasa,  
Jl. Jend. Sudirman. Km. 3. Cilegon. Banten. 42435, Indonesia.  
Email: teguhfirmansyah@untirta.ac.id

## 1. INTRODUCTION

In recent years, microstrip patch antenna technology is widely used. The microstrip patch antenna has advantages such as low fabrication cost, light in weight, capable of supporting multiple frequency bands, easily etched on any PCB and integrated them with MICs or MMICs [1-3]. However, it has disadvantages such as low gain, large PCB structure, and narrow bandwidth due to conductor losses, surface wave losses,

and dielectric losses [4, 5]. Several studies investigating bandwidth enhancement of microstrip antenna have been carried out by [6, 7]. The proposed methods include defected ground structure (DGS) [6], electromagnetic band gap (EBG) [7, 8], parasitic patch [9, 10], metamaterial [11], metamaterial bilayer substrates (MBS) [12], monopole slot [13], T-shaped slot [14], cylindrical dielectric slot (CDS) [15], polymeric grid [16], spiral split ring (SSR) [17], Jerusalem cross-shaped [18], and characteristic modes [19].

The DGS method was proposed by Marotkar [6], it is realized by etching the ground plane so the current distribution in the ground plane is disturbed. As the results, the antenna has a wide bandwidth of 302 MHz with center frequency of 2.4 GHz, and reflection coefficient of -23.26 dB. Furthermore, Gupta [7] and Hadarig [8] investigated bandwidth enhancement of microstrip patch antennas by implementing EBG structures. This proposed antenna has a center frequency of 10 GHz and 2.4 GHz for X-band Radar and VHF RFID, respectively. Then, to reduce the size of the antenna, Rothwell and Raoul O [21] proposed a metamaterial structure. The metamaterial microstrip structure has advantages such as compact size and broadband. However, the structure has complex geometry, and it is difficult to fabricate. Then, H. Mosallaei and K. Sarabandi [22] proposed bandwidth enhancement by using a reactive impedance substrate (RIS). This method succeeds to increase the bandwidth of the antenna and reduce antenna size.

Moreover, a fascinating method was proposed by Mohamadi [18]. It investigated the bandwidth enhancement of antenna for Long Term Evolution (LTE) technology with multiple input multiple output (MIMO) application. He introduced the basic modes method, this method successfully to enhance the bandwidth of the antenna, but it was still a drawback such as complex microstrip structure. Other methods include, G-shaped band-notched antenna [23], dielectric resonator antenna (DRA) [24], and U-shaped slot antenna [25]. The DRA antenna that is proposed by [24] has good bandwidth. However, the antenna structure is still large.

As the novelty, to enhance bandwidth and reduce antenna size, beveled half-cut microstrip structure is proposed in this paper. Further, this proposed antenna structure will be applied to multiple input multiple output (MIMO) antenna 2×2. Therefore, this research was investigated conventional circular shape antenna (CCSA), circular shaped beveled antenna (CSBA), and MIMO circular shaped beveled antenna (MIMO-CBSA) as Model 1, Model 2, and Model 3, respectively. An FR4 substrate with  $\epsilon_r=4.4$ , thickness  $h=1.6$  mm, and  $\tan \delta=0.0265$  was used. In brief, Table 1. provides the research position of this paper compare to another research of bandwidth enhancement and miniaturization of the antenna.

Table 1. The Research Position of Bandwidth Enhancement and Miniaturization of the Antenna

Ref. no	Method	Center Freq.	Wireless Technology	Bandwidth Enhancement	Miniaturization	MIMO Application
[6]	DGS	2.4 GHz	WLAN	yes	-	-
[7]	EBG	10 GHz	X-band Radar	yes	-	-
[8]	EBG	2.4 GHz	RFID	yes	-	-
[9]	Parasitic Patch	8.5 GHz	X-band	yes	-	-
[10]	Parasitic Patch	120 MHz	VHF RFID	yes	-	-
[11]	Metamaterial	1.9 GHz	GSM	yes	-	-
[12]	Metamaterial Bilayer	2.6 GHz	LTE	yes	-	-
[13]	Monopole Slot	4.4 GHz	WiMAX	yes	-	-
[14]	T-shaped Slot	6.7 GHz	UWB	yes	-	-
[15]	Dielectric Slot	11.25 GHz	X-band	yes	-	-
[16]	Polymeric Grid	26.8 GHz	5G	yes	-	-
[17]	Spiral Split Ring	5.8 GHz	WLAN	yes	-	-
[18]	Jerusalem Cross-Shaped	5.8 GHz	WLAN	yes	-	-
[19]	Characteristic Modes	1.9 GHz	LTE	yes	-	yes
[20]	Parasitic Patch	2.6 GHz	LTE	yes	-	yes
[21]	Metamaterial	2.6 GHz	LTE	-	yes	-
[22]	RIS	1.9 GHz	WCDMA	yes	yes	-
[23]	G-shaped band-notched	7.75 GHz	UWB	-	-	yes
[24]	DRA	30 GHz	5G	-	-	yes
[25]	U-shaped Slot	3 GHz	Selular	-	-	yes
This paper	Circular-Shaped with Beveled Halfcut Structure	2.175 GHz	GSM, WCDMA, LTE, and WLAN	yes	yes	yes

This rest of this paper is detailed as follows. In Section 2, the proposed circular shaped beveled antenna and MMO circular shaped beveled antenna are presented. The detail of numerical simulation was also described in Section 2. Furthermore, the measurement results of the fabricated antenna and the comparison with simulation result was explained in Section 3. Finally, Section 4 concludes this research.

**2. RESEARCH METHOD**

In this section, the proposed circular shaped beveled antenna and MMO circular shaped beveled antenna were designed. Figure 1(a), Figure 1(b), Figure 1(c), Figure 1(d), and Figure 1(e) show conventional circular shape antenna (CCSA) [Model-1], front view of CCSA, circular shaped beveled antenna (CSBA) [Model-2], front view of CSBA, MIMO circular shaped beveled antenna (CSBA) [Model-3], respectively.

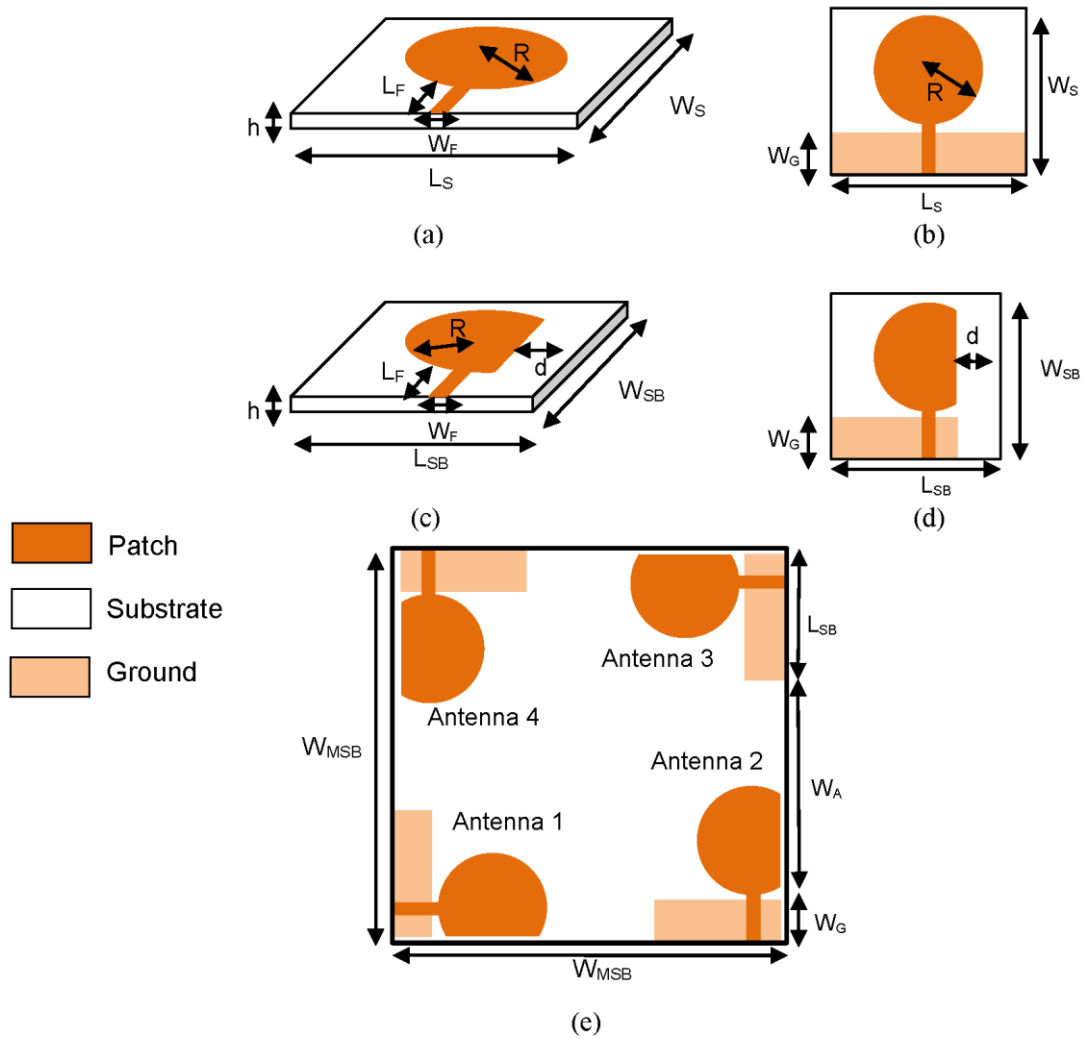


Figure 1. (a) Conventional Circular Shape Antenna (CCSSA) [Model-1], (b) Front view of Conventional Circular Shape Antenna, (c) Circular Shaped Beveled Antenna (CSBA) [Model-2], (d) Front view of Circular Shaped Beveled Antenna, (e) MIMO Circular Shaped Beveled Antenna (MIMO-CSBA) [Model-3]

The radius of circular-shaped microstrip patch antenna is formulated by [26], [27]:

$$R = \frac{F}{\sqrt{1 + \frac{2h}{\pi\epsilon_r} \left[ \ln\left(\frac{\pi F}{2h}\right) + 1.7726 \right]}} \tag{1}$$

Where

$$F = \frac{8.791 \times 10^9}{f_r \sqrt{\epsilon_r}} \tag{2}$$

with  $h$ =thickness of substrate (cm),  $\epsilon_r$ =permittivity of substrate, and  $f_r$ =resonant frequency (Hz). A direct feeding method was used in this paper. Moreover, the impedance characteristic ( $Z_0$ ) can be determined by the ratio of a thickness of substrate ( $h$ ) and its width ( $W$ ) [28].

When  $Z_0\sqrt{\epsilon_{re}} > 89.91$ ,  $W/h$  ratio is given by [29], [30]:

$$W/h = \frac{8 \exp(A)}{\exp(2A) - 2} \quad (3)$$

when  $Z_0\sqrt{\epsilon_{re}} \leq 89.91$ ,  $W/h$  ratio is given by [29], [30]:

$$W/h = \frac{2}{\pi} \left\{ B - 1 - \ln(2B - 1) + \frac{\epsilon_r - 1}{2\epsilon_r} \left[ \ln(B - 1) + 0.39 - \frac{0.61}{\epsilon_r} \right] \right\} \quad (4)$$

where

$$A = \frac{Z_0}{60} \left\{ \frac{\epsilon_r + 1}{2} \right\}^{1/2} + \frac{\epsilon_r - 1}{\epsilon_r + 1} \left\{ 0.23 + \frac{0.11}{\epsilon_r} \right\} \quad (5)$$

$$B = \frac{60\pi^2}{Z_0\sqrt{\epsilon_r}} \quad (6)$$

$$\epsilon_{re} = \frac{\epsilon_r + 1}{2} + \frac{\epsilon_r - 1}{2} F \left( \frac{W}{h} \right) \quad (7)$$

Furthermore, the conductivity loss ( $\alpha_c$ ) of microstrip transmission line feeding is given by [29], [30];

$$\alpha_c = \begin{cases} 1,38D \frac{R_s}{hZ_0} \frac{32 - (W/h)^2}{32 + (W/h)^2} & \left( \frac{W}{h} \leq 1 \right) \\ 6,1 \times 10^{-5} D \frac{R_s Z_0 \epsilon_{re}(f)}{h} \left[ W_e/h + \frac{0,667 W/h}{W_e/h + 1,444} \right] & \left( \frac{W}{h} \geq 1 \right) \end{cases} \quad (8)$$

where

$$D = 1 + \frac{h}{W} \left\{ 1 + \frac{1,25}{\pi} \ln \frac{4\pi W}{t} \right\} \quad (9)$$

with

$$R_s = \sqrt{\pi f \mu_0 \rho_c},$$

$\rho_c$  = resistivity of the conductor,

$f$  = frequency (Hz), and

$\mu_0 = 4\pi \times 10^{-7} \text{ N}\cdot\text{A}^{-2}$  is the magnetic permeability of free space,

The numerical simulation of the antenna parameters has been conducted by using Advanced Design System (ADS). The FR4 substrate with  $\epsilon_r=4.4$ , thickness  $h=1.6$  mm, and  $\tan \delta=0.0265$  was used. Figure 2(a) shows the extracted reflection coefficient with varied  $R$ . The data shows that by modifying the radius ( $R$ ), the reflection coefficient can be tuned. However, for  $R=22$  mm and  $R=24$  mm, the antenna is not resonance. Furthermore, Figure 2(b) shows the voltage standing wave ratio (VSWR) value by varied radius ( $R$ ). The simulation result shows that VSWR value is better than 2 at  $R=28$  mm and  $R=30$  mm.

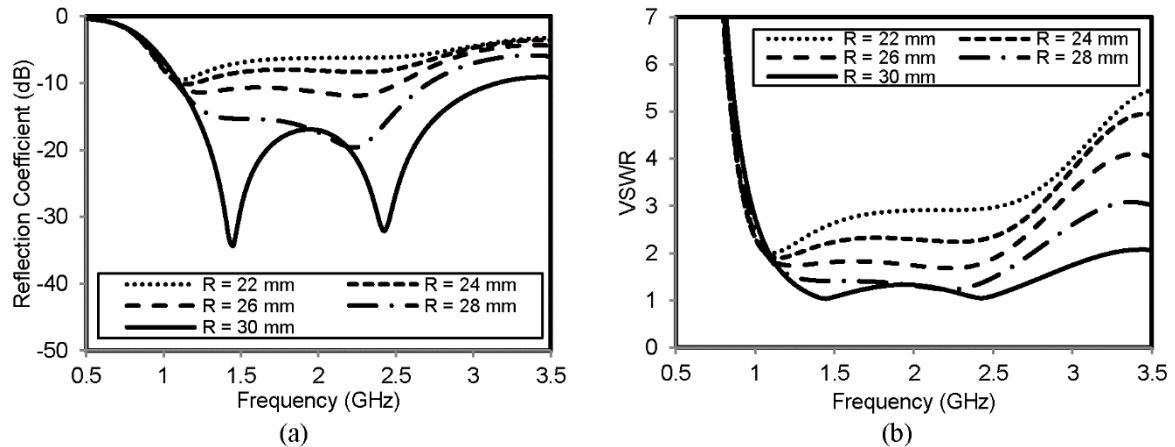


Figure 2. (a) The extracted reflection coefficient with varied R (mm); (b) The extracted voltage standing wave ratio (VSWR) with varied R (mm)

Figure 3(a) and Figure 3(b) illustrate the reflection coefficient with varied  $W_G$  and voltage standing wave ratio (VSWR) with varied  $W_G$ , respectively. From the data in Figure 3(a), we can see that the  $W_G$  is essential parameters to make the antenna resonate. The Figure 3(a) shows that by increasing the  $W_G$  (mm), the antenna will be more resonate. Moreover, Figure 3(b) shows clearly trend that the VSWR of the antenna is better than 2 (two) for  $W_G$  is longer than 28 mm. However, the dimension of this antenna is large. The next step explains the miniaturization process.

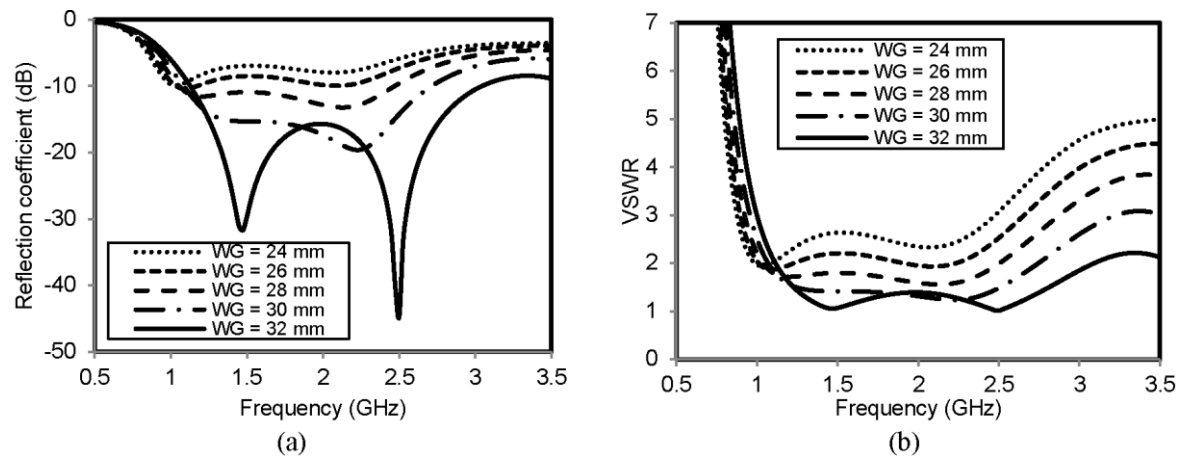


Figure 3. (a) The extracted reflection coefficient with varied  $W_G$  (mm); (b) The extracted voltage standing wave ratio (VSWR) with varied  $W_G$  (mm)

In this paper, the bandwidth enhancement and miniaturization of the antenna is obtained by the beveled method as shown in Figure 1(b) and Figure 1(c). The beveled method was applied by cut one side of the antenna, partially. Furthermore, the size of the antenna will be reduced by  $d$  (mm). Moreover, the result of numerical simulation based on the beveled method is depicted in Figure 4(a) and Figure 4(b). Figure 4(a) illustrates the extracted reflection coefficient with varied  $d$  (mm). Base on Figure 4(a), the data shows that at  $d=10$  mm produce large bandwidth. However for  $d=10$  mm at the frequency of 2.8 GHz, the reflection coefficient is higher than -10 dB at frequency of 2.8 GHz. Therefore, the value  $d=10$  mm is not chosen because the reflection coefficient is too high. Therefore, the data shows that the largest bandwidth is generated at  $d=8$  mm. This result is also indicated in Figure 4(b) which presents the extracted center frequency and bandwidth with varied  $d$  (mm). For instance, the circular shaped beveled antenna (CSBA) [Model-2] is represented by the antenna with  $d=8$  mm and the conventional circular shape antenna (CCSA) [Model-1] is represented by the antenna with  $d=0$  mm.

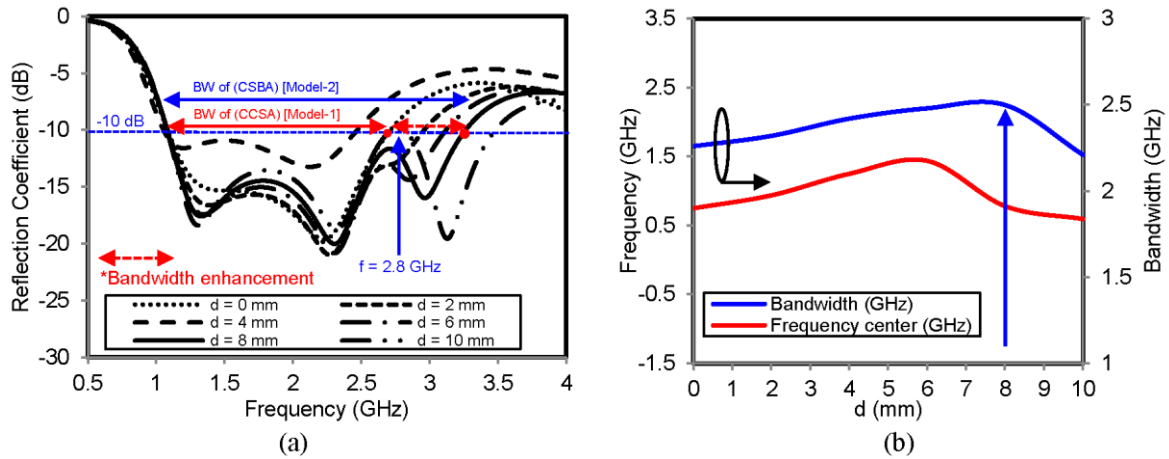


Figure 4. (a) The extracted reflection coefficient with varied d (mm); (b) The extracted frequency center and bandwidth with varied d (mm)

The next step is to apply the CSBA [Model-2] to MIMO-CSBA [Model-3] antenna as shown in Figure 1(e). Furthermore, Figure 5(a) shows the extracted reflection coefficient with different  $W_{SMB}$  (mm) and Figure 5(b) illustrates the extracted voltage standing wave ratio (VSWR) with varied  $W_{SMB}$  (mm). Figure 5(a) shows a clear illustration that the reflection coefficient is stable for the different length of  $W_{SMB}$  and it shows that the reflection coefficient values are lower than -10 dB. However, the reflection coefficient for  $W_{SMB}=180$  mm generates lower bandwidth than others. Furthermore, it appears from Figure 5(b) that the VSWR values are still lower than 2 (two). This data shows that the antenna is working properly with good performance.

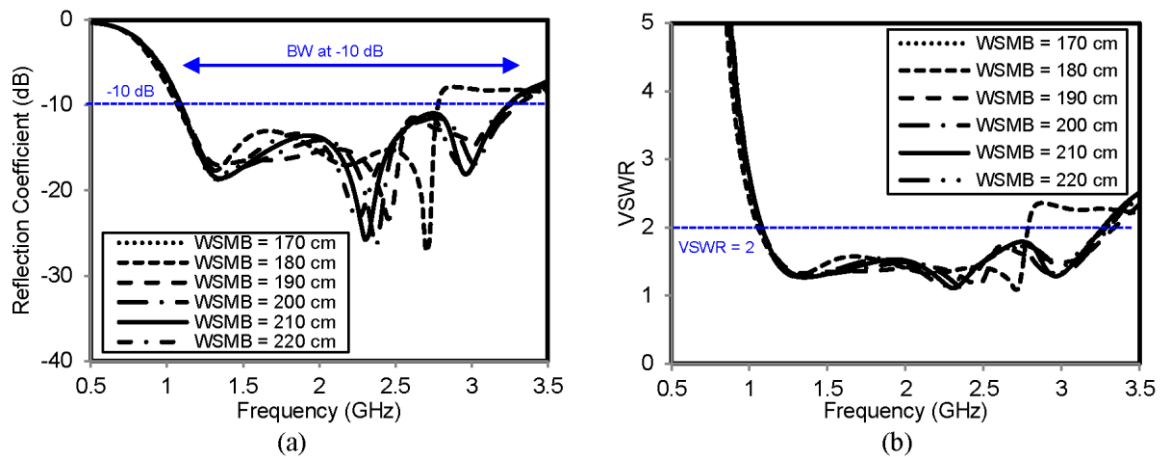


Figure 5. (a) The extracted reflection coefficient with varied  $W_{SMB}$  (mm); (b) The extracted voltage standing wave ratio (VSWR) with varied  $W_{SMB}$  (mm)

The numerical simulation result of mutual coupling MIMO antenna is shown in Figure 6(a) and Figure 6(b). Figure 6(a) exhibits the extracted mutual coupling ( $S_{21}$ ) with varied  $W_{SMB}$  (mm) and Figure 6(b) illustrates the extracted mutual coupling ( $S_{31}$ ) with varied  $W_{SMB}$  (mm). The mutual coupling value of  $S_{21}$  (dB) and  $S_{31}$  (dB) demonstrate the coupling between Antena 1 to Antena 2 and Antena 1 to Antena 3, respectively. The coupling coefficient is lower than -15 dB almost over the whole band which shows a good isolation performance. However, the coupling coefficient for  $W_{SMB}=180$  mm is higher than -15 dB at the frequency of 2.8 GHz. So, the  $W_{SMB}=180$  mm cannot be chosen. The distance between antenna effects on mutual coupling. The mutual coupling can be decreased by increasing the distance between the MIMO antennas. However, the size of the antennas cannot be made too large.

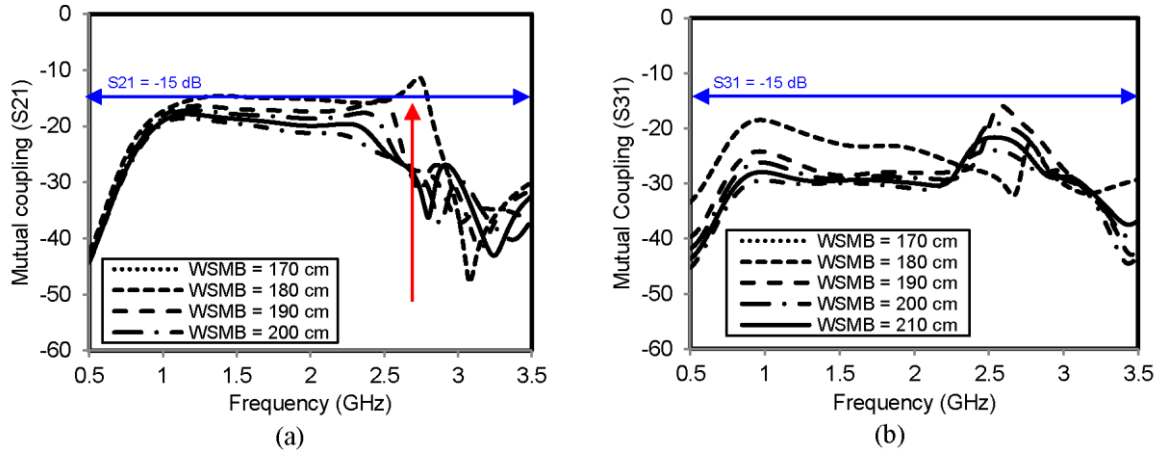


Figure 6. (a) The extracted mutual coupling ( $S_{21}$ ) with varied  $W_{SMB}$  (mm); (c) The extracted mutual coupling ( $S_{31}$ ) with varied  $W_{SMB}$  (mm)

3. RESULTS AND ANALYSIS

To verify the simulation result, the measurement of the antenna prototype must be carried out. The photograph of the fabricated proposed antenna is depicted in Figure 7(a), Figure 7(b), and Figure 7(c). Figure 7(a) shows the photograph of conventional circular shape antenna (CCSA) [Model-1], and Figure 7(b) illustrates the photograph of circular shaped beveled antenna (CSBA) [Model-2]. Furthermore, Figure 7(c) presents the photograph MIMO circular shaped beveled antenna (MCSBA) [Model-3]. The FR4 substrate with  $\epsilon_r=4.4$ , thickness  $h=1.6$  mm, and  $\tan d=0.0265$  was used. The simulation and optimization has been conducted using Advanced Design System (ADS). The detailed geometric parameters are  $R=28$  mm,  $L_S=63$  mm,  $W_S=90$  mm,  $W_G=30$  mm,  $L_F=34$  mm,  $W_F=3$ mm,  $d=8$  mm,  $L_{SB}=51.5$  mm,  $W_{SB}=90$  mm,  $W_{MSB}=190$  mm, and  $W_A=98.5$  mm, Moreover, the full size of the PCB board is  $190 \times 190$  mm<sup>2</sup>.

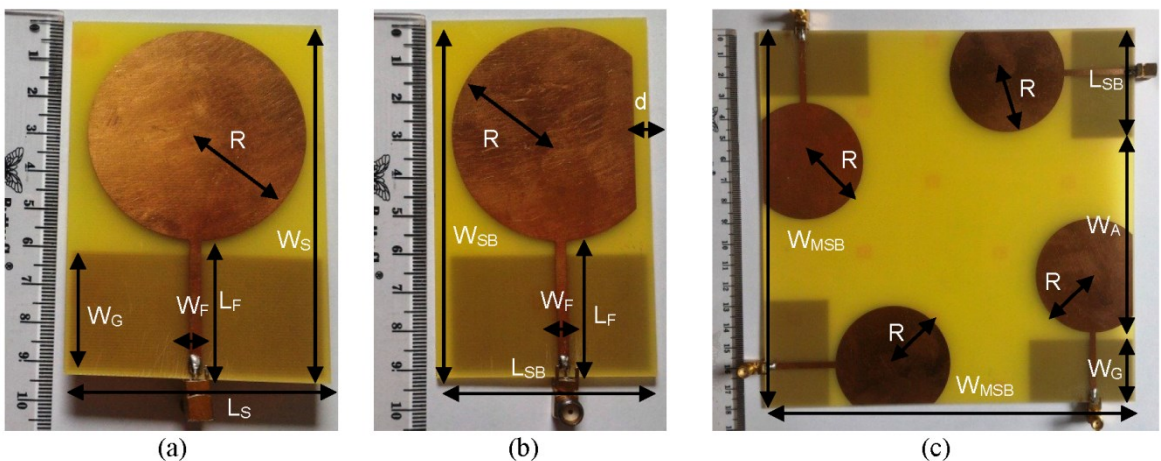


Figure 7. Photograph of (a) conventional circular shape antenna (CCSA) [Model-1], (b) circular shaped beveled antenna (CSBA) [Model-2], (c) MIMO circular shaped beveled antenna (MCSBA) [Model-3]

Figure 8(a) shows the comparison between simulated and measured of reflection coefficient of CCSA antenna dan CSBA antenna. The simulated/measured of CCSA antenna [Model-1] achieves lower frequency=1.093 GHz/1.094 GHz, upper frequency=2.719 GHz/2.568 GHz, center frequency=1.906 GHz/1.831 GHz, bandwidth=1.626 GHz/1.474 GHz, and reflection coefficient=-16.39 dB/-15.13 dB with the size of CCSA antenna has 63x90 mm. Furthermore, the simulated/measured of CBSA antenna [Model-2] achieves lower frequency=1.051 GHz/1.090 GHz, upper frequency=3.299 GHz/3.422 GHz, center frequency=2.175 GHz/2.265 GHz, bandwidth=2.248 GHz/2.332 GHz, and reflection



coefficient=-17.99 dB/17.37 dB with the size of CSBA antenna has 51.5x90 mm. Moreover, Figure 8(b) shows the comparison between simulated and measured of VSWR. The simulated/measured of CCSA antenna [Model-1] achieves VSWR=1.35/1.42, and the simulated/measured of CSBA antenna [Model-2] achieves VSWR=1.28/1.31. Base on the measurement performance, both antennas can work as expected. However, the comparison result showed that proposed antenna CSBA [Model 2] has wider-bandwidth of 58,2% and smaller-size of 18.2%.

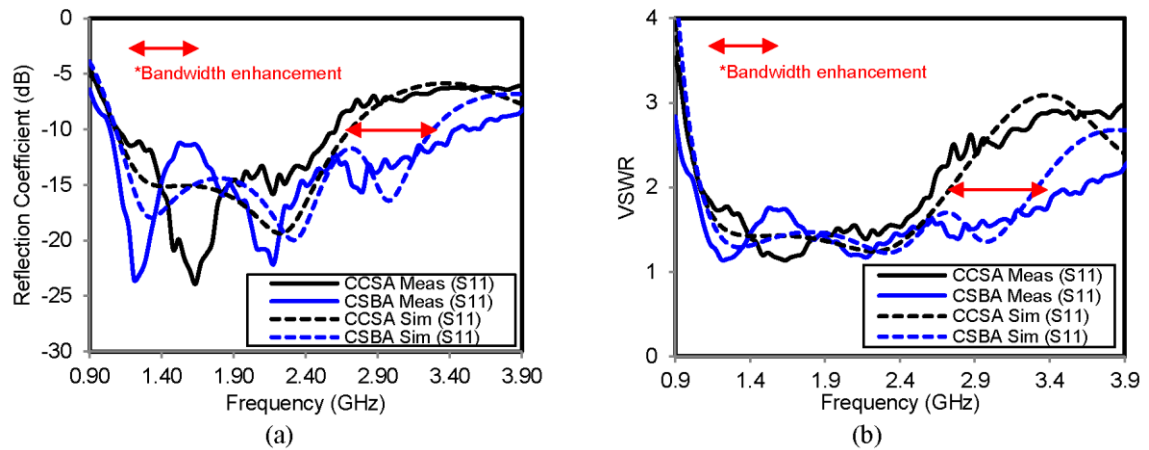


Figure 8. (a) The comparison between simulated and measured of reflection coefficient; (b) The comparison between simulated and measured of VSWR

Figure 9(a) exhibits the comparison of gain (dBi), directivity (dBi), efficiency (%). The gain of CCSA [Model 1]/CSBA [Model 2] antenna has 1.58 dBi/1.56 dBi, 3.61 dBi/2.29 dBi, 2.44 dBi/2.27 dBi, and 2.47 dBi/2.34 dBi for frequency of 0.95 GHz, 1.85 GHz, 2.35 GHz, and 2.45 GHz, respectively. Furthermore, the directivity of CCSA [Model 1]/CSBA [Model 2] antenna has 2.34 dBi/2.32 dBi, 2.36 dBi/3.54 dBi, 3.99 dBi/3.74 dBi, and 4.09 dBi/3.84 dBi for frequency of 0.95 GHz, 1.85 GHz, 2.35 GHz, and 2.45 GHz, respectively. The efficiency of CCSA [Model 1]/CSBA [Model 2] antenna has 83.99 %/83.92%, 75.12 %/74.92%, 70.10%/71.25%, and 68.95%/70.89% for frequency of 0.95 GHz, 1.85 GHz, 2.35 GHz, and 2.45 GHz, respectively. Moreover, Figure 9(b) shows the comparison between simulated and measured of mutual coupling ( $S_{21}$ ) and ( $S_{31}$ ). The simulated/measured of mutual coupling of MIMO-CBSA [Model-3] antenna are -16.15 dB/-26.18 dB and -27.11 dB/-26.41 dB for mutual coupling ( $S_{21}$ ) and mutual coupling ( $S_{31}$ ), respectively. The MIMO antenna obtain very good mutual coupling (<-15dB). Moreover, the measured results are in a good agreement with the simulated results.

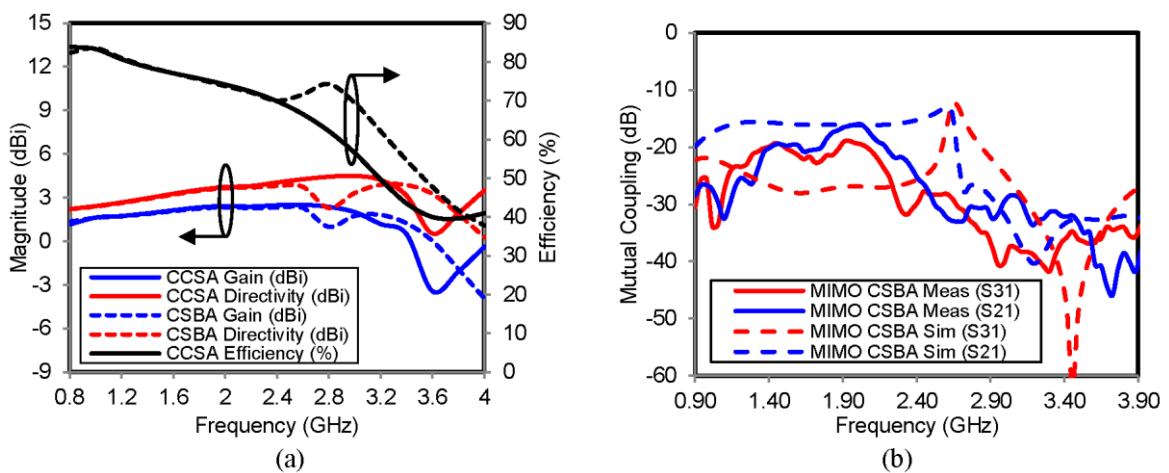


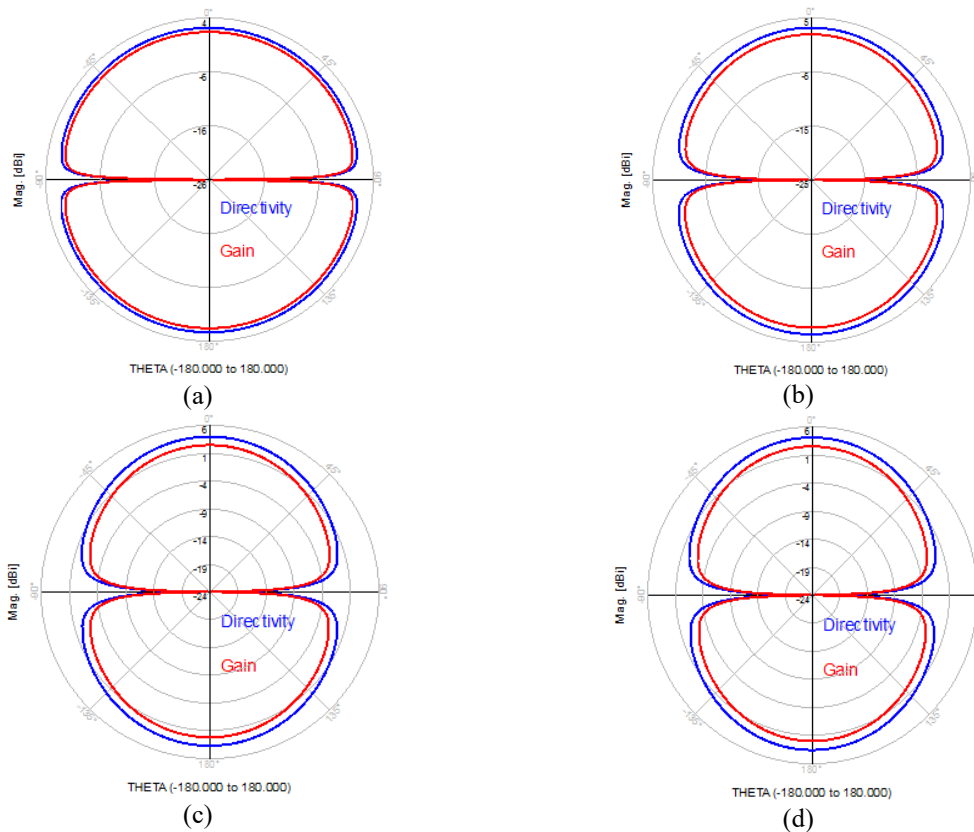
Figure 9. (a) The comparison gain (dBi), directivity (dBi), Efficiency (%), (b) The comparison between simulated and measured of mutual coupling ( $S_{21}$ ) and ( $S_{31}$ )



Table 2 summarizes the comparison of simulated and measured data of CCSA [Model-1] antenna, CSBA [Model-2] antenna, and MIMO CSBA [Model-3] antenna, in brief. Moreover, the radiation patterns of the proposed antenna are shown in Figure 10(a)-(h). In conclusion, all of these advantages make it particularly valuable in multistandard antenna applications design such as GSM950, WCDMA1800, LTE2300, and WLAN2400.

Table 2. The Comparison of Simulated and Measured Result of CCSA [Model-1] Antenna, CSBA [Model-2] Antenna, and MIMO CSBA [Model-3] Antenna

Performace	CCSA [Model-1]		CSBA [Model-2]		MIMO CSBA [Model-3]		
	Simulated	Measured	Simulated	Measured	Simulated	Measured	
Lower frequency (GHz)	1.093	1.094	1.051	1.090	1.061	1.095	
Upper frequency (GHz)	2.719	2.568	3.299	3.422	3.275	3.417	
Center frequency (GHz)	1.906	1.831	2.175	2.265	2.168	2.256	
Bandwidth (MHz)	1.626	1.474	2.248	2.332	2.214	2.322	
Reflection coefficient (dB)	-16.39	-15.13	-17.99	-17.37	-17.12	-17.25	
VSWR	1.35	1.42	1.28	1.31	1.32	1.33	
Mutual coupling (S <sub>21</sub> )	NA	NA	NA	NA	-16.15	-26.18	
Mutual coupling (S <sub>31</sub> )	NA	NA	NA	NA	-27.11	-26.41	
Gain @ f=0.95 GHz (dBi)	1.58	NA	1.56	NA	0.14	NA	
Gain @ f=1.85 GHz (dBi)	3.61	NA	2.29	NA	3.90	NA	
Gain @ f=2.35 GHz (dBi)	2.44	NA	2.27	NA	4.64	NA	
Gain @ f=2.45 GHz (dBi)	2.47	NA	2.34	NA	4.84	NA	
Directivity @ f=0.95 GHz (dBi)	2.34	NA	2.32	NA	1.47	NA	
Directivity @ f=1.85 GHz (dBi)	2.36	NA	3.54	NA	4.50	NA	
Directivity @ f=2.35 GHz (dBi)	3.99	NA	3.74	NA	5.49	NA	
Directivity @ f=2.45 GHz (dBi)	4.09	NA	3.84	NA	5.16	NA	
Efficiency @ f=0.95 GHz (%)	83.99	NA	83.92	NA	73.74	NA	
Efficiency @ f=1.85 GHz (%)	75.12	NA	74.92	NA	87.25	NA	
Efficiency @ f=2.35 GHz (%)	70.10	NA	71.25	NA	82.23	NA	
Efficiency @ f=2.45 GHz (%)	68.95	NA	70.89	NA	92.82	NA	
Size	W (mm)	63	63	51.5	51.5	190	190
	L (mm)	90	90	90	90	190	190
	H (mm)	1.6	1.6	1.6	1.6	1.6	1.6



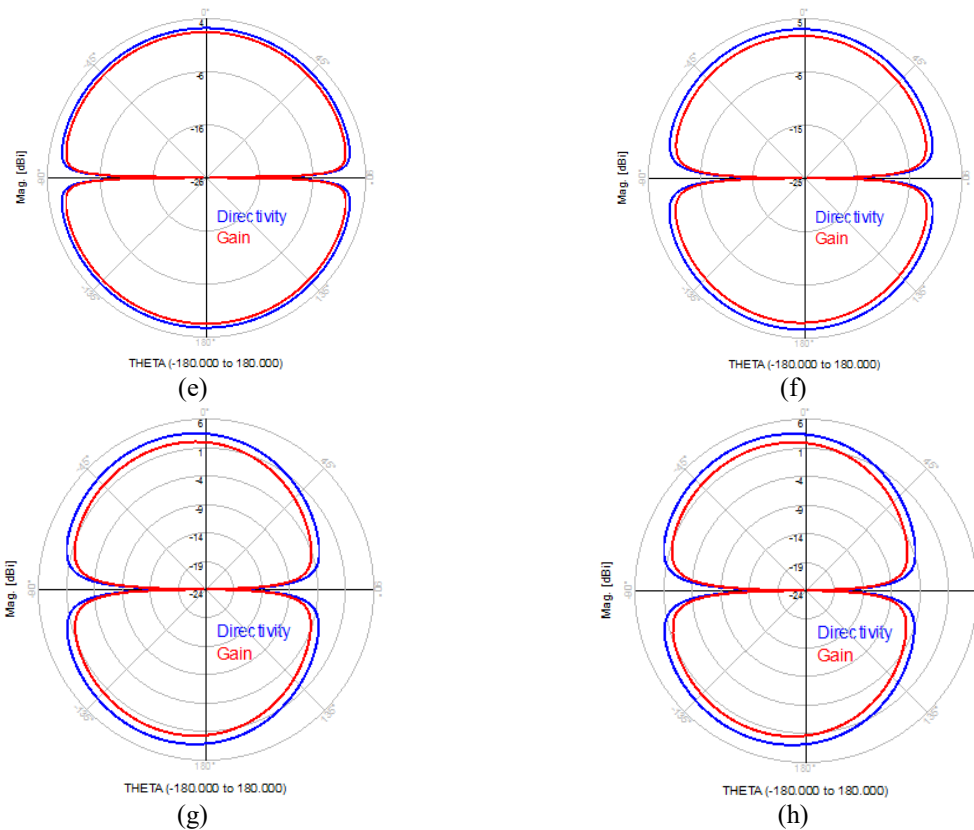


Figure 10. Gain and directivity of CCSA at frequency (a)  $f=0.95$  GHz, (b)  $f=1.85$  GHz, (c)  $f=2.35$  GHz, (d)  $f=2.45$  GHz. Gain and directivity of CSBA at frequency (e)  $f=0.95$  GHz, (f)  $f=1.85$  GHz, (g)  $f=2.35$  GHz, (h)  $f=2.45$  GHz

#### 4. CONCLUSION

In order to reduce the antenna size and enhance the bandwidth of antenna, this paper was proposed the beveled half-cut microstrip structure. Moreover, this research was investigated conventional circular shape antenna (CCSA), circular shaped beveled antenna (CSBA), and MIMO circular shaped beveled antenna (MIMO-CBSA) as Model 1, Model 2, and Model 3, respectively. This antenna was fabricated on FR4 substrate with  $\epsilon_r=4.4$ , thickness  $h=1.6$  mm, and  $\tan \delta=0.0265$ . The numerical simulation has been conducted using Advanced Design System (ADS). The measured result showed that proposed antenna CSBA [Model 2] has wider-bandwidth of 58,2% and smaller-size of 18.2% compared to CCSA [Model 1] antenna. Then, after CSBA [Model 2] structure was applied to MIMO  $2 \times 2$  [Model 3], the MIMO antenna obtain very good mutual coupling ( $< -15$ dB). Moreover, the measured results are good agreement with the simulated results. In conclusion, all of these advantages make it particularly valuable in multistandard antenna applications design such as GSM950, WCDMA1800, LTE2300, and WLAN2400.

#### ACKNOWLEDGEMENTS

The authors thank the LPPM Universitas Sultan Ageng Tirtayasa (UNTIRTA) and Ministry of Research, Technology and Higher Education, Indonesian Government, KEMENRISTEK DIKTI for the financial support.

#### REFERENCES

- [1] L. Wang, Z. Weng, Y. C. Jiao, W. Zhang and C. Zhang, "A Low-Profile Broadband Circularly Polarized Microstrip Antenna With Wide Beamwidth," *IEEE Antennas and Wireless Propagation Letters*, vol. 17, no. 7, pp. 1213-1217, July 2018. doi: 10.1109/LAWP.2018.2839100
- [2] Hashim Dahri, et al. "Broadband Resonant Elements for 5G Reflectarray Antenna Design," *TELKOMNIKA Telecommunication Computing Electronics and Control*, vol. 15 (3), pp. 793-798. 2017.

- [3] Raimi Dewanet., et al "Dual Band to Wideband Pentagon-shaped Patch Antenna with Frequency Reconfigurability using EBGs," *International Journal of Electrical and Computer Engineering (IJECE)*, Vol.8, No.4, pp. 2557-2563. August 2018.
- [4] E. Ragab M, "Study on Bandwidth Enhancement Techniques of Microstrip Antenna," *Journal of Electrical Systems and Information Technology*, vol. 3 (3), pp. 527-531, December 2016. doi: 10.1016/j.jesit.2015.05.003
- [5] J. F. Lin and Q. X. Chu, "Enhancing Bandwidth of CP Microstrip Antenna by Using Parasitic Patches in Annular Sector Shapes to Control Electric Field Components," *IEEE Antennas and Wireless Propagation Letters*, vol. 17, no. 5, pp. 924-927, May 2018. doi: 10.1109/LAWP.2018.2825236
- [6] D. S. Marotkar and P. Zade, "Bandwidth Enhancement of Microstrip Patch Antenna Using Defected Ground Structure," *International Conference on Electrical, Electronics, and Optimization Techniques (ICEEOT)*, Chennai, pp. 1712-1716, 2016. doi: 10.1109/ICEEOT.2016.7754978.
- [7] Gupta and M. Kumar, "Bandwidth Enhancement of Microstrip Patch Antennas by Implementing Electromagnetic Bandgap (EBG) Structures," *Fourth International Conference on Computational Intelligence and Communication Networks*, Mathura, pp. 15-18, 2012. doi: 10.1109/CICN.2012.58
- [8] R. C. Hadarig, M. E. de Cos, and F. Las-Heras., "Microstrip Patch Antenna Bandwidth Enhancement Using AMC/EBG Structures," *International Journal of Antennas and Propagation*, vol. pp. 1-6, 2012. doi:10.1155/2012/843754
- [9] M. H. Reddy, R. M. Joany, M. J. Reddy, M. Sugadev and E. Logashanmugam, "Bandwidth Enhancement of Microstrip Patch Antenna Using Parasitic Patch," *IEEE International Conference on Smart Technologies and Management for Computing, Communication, Controls, Energy and Materials (ICSTM)*, Chennai, pp. 295-298, 2017. doi: 10.1109/ICSTM.2017.8089172
- [10] Lin Peng, Fu-Man Yang and Xing Jiang, "Simple and Electrically Small EZR-MZR Resonator With Quasi-Isotropic Pattern," *IEEE Journal of Radio Frequency Identification*, vol. 1, 2017. doi: 10.1002/mop.30471
- [11] P. Ananya., et al., "Bandwidth Enhancement of Microstrip Patch Antenna Using Metamaterials," *IOSR Journal of Electronics and Communication Engineering (IOSR-JECE)*, vol. 8 (4), pp. 5-10. Nov 2013
- [12] R. Yang , Y. Xie , D. Li , J. Zhang & J. Jiang. "Bandwidth Enhancement of Microstrip Antennas with Metamaterial Bilayered Substrates", *Journal of Electromagnetic Waves and Applications*, vol. 21(15), pp. 2321-2330, 2007. doi: 10.1163/156939307783134425
- [13] B. Sudeep, V. Dinesh Kumar., "Bandwidth Enhancement of a Planar Monopole Microstrip Patch Antenna," *International Journal of Microwave and Wireless Technologies*. vol. 8, issue 2, pp. 237-242. March 2016. doi:10.1017/S175907871400141X
- [14] S. Kun Song, Y. Ying-Zeng, Xiao-Bo Wu, and Li Zhang., "Bandwidth Enhancement of Open Slot Antenna With A T-Shaped Stub," *Microwave And Optical Technology Letters*. vol. 52,no. 2, pp. 390-393. February 2010. doi: 10.1002/mop
- [15] M. Nipun K, D. Soma, and V. Dinesh K., "Bandwidth Enhancement of Cylindrical Dielectric Resonator Antenna Using Thin Dielectric Layer Fed by Resonating Slot". *Frequenz*. Vol. 70, pp. 381–388. 2016. doi: 10.1515/freq-2015-0188
- [16] M. Wan Asilah Wan., "Bandwidth enhancement using Polymeric Grid Array Antenna for millimeter-wave application". *Appl. Phys. A*. vol. 123:69, 2017 doi: 10.1007/s00339-016-0689-0
- [17] Arora C., Pattnaik S.S., Baral R.N. (2018) Bandwidth Enhancement of Microstrip Patch Antenna Array Using Spiral Split Ring Resonator. *Advances in Intelligent Systems and Computing*, vol 672. doi:10.1007/978-981-10-7512-4
- [18] F. Mohamadi Monavar and N. Komjani., "Bandwidth Enhancement Of Microstrip Patch Antenna Using Jerusalem Cross-Shaped Frequency Selective Surfaces By Invasive Weed Optimization Approach". *Progress In Electromagnetics Research*, vol. 121, pp. 103-120, 2011.
- [19] Z. Miers, H. Li and B. K. Lau, "Design of Bandwidth-Enhanced and Multiband MIMO Antennas Using Characteristic Modes," *IEEE Antennas and Wireless Propagation Letters*, vol. 12, pp. 1696-1699, 2013. doi: 10.1109/LAWP.2013.2292562
- [20] Y. Wen, D. Yang, H. Zeng, M. Zou and J. Pan, "Bandwidth Enhancement of Low-Profile Microstrip Antenna for MIMO Applications," *IEEE Transactions on Antennas and Propagation*, vol. 66, no. 3, pp. 1064-1075, March 2018. doi: 10.1109/TAP.2017.2787542
- [21] Edward J. Rothwell and Raoul O. Ouedraogo., "Antenna Miniaturization: Definitions, Concepts, and a Review With Emphasis on Metamaterials," *Journal of Electromagnetic Waves and Applications*, doi: 10.1080/09205071.2014.972470
- [22] H. Mosallaei and K. Sarabandi, "Antenna Miniaturization and Bandwidth Enhancement Using a Reactive Impedance Substrate," *IEEE Transactions on Antennas and Propagation*, vol. 52, no. 9, pp. 2403-2414, Sept. 2004. doi: 10.1109/TAP.2004.834135
- [23] A. Toktas, "G-shaped Band-Notched Ultra-Wideband MIMO Antenna System for Mobile Terminals," *IET Microwaves, Antennas & Propagation*, vol. 11, no. 5, pp. 718-725, 2017. doi: 10.1049/iet-map.2016.0820
- [24] M. S. Sharawi, S. K. Podilchak, M. T. Hussain and Y. M. M. Antar, "Dielectric Resonator based MIMO Antenna System Enabling Millimetre-Wave Mobile Devices." *IET Microwaves, Antennas & Propagation*, vol. 11, no. 2, pp. 287-293, 1 29. 2017. doi: 10.1049/iet-map.2016.0457
- [25] H. T. Hu, F. C. Chen and Q. X. Chu, "A Wideband U-Shaped Slot Antenna and Its Application in MIMO Terminals," *IEEE Antennas and Wireless Propagation Letters*, vol. 15, pp. 508-511, 2016. doi: 10.1109/LAWP.2015.2455237

- [26] T Pramendra, P Sharma, T Bandopadhyay. "Gain Enhancement of Circular Microstrip Antenna for Personal Communication Systems," *International Journal of Engineering and Technology*. vol. 3(2), pp. 175-178. 2011.
- [27] Firmansyah, T. et al., "Bandwidth and Gain Enhancement of MIMO Antenna by Using Ring and Circular Parasitic With Air-Gap Microstrip Structure," *TELKOMNIKA Telecommunication Computing Electronics and Control*. vol. 15 (3), pp. 1155-1163. 2017.
- [28] Firmansyah, T. et al., "Dual-Wideband Band Pass Filter Using Folded Cross-Stub Stepped Impedance Resonator," *Microwave and Optical Technology Letters*, vol. 59 (11), pp. 2929-2934, November 2017.
- [29] Bahl, Inder, *Lumped Elements for RF and Microwave Circuits*. Norwood: Artech House, Inc, 2003.
- [30] D. Pozar *Microwave Engineering*, Fourth Edition, Wiley, 2011.